

BUILDING SIMULATION OF ENERGY CONSUMPTION AND AMBIENT TEMPERATURE : APPLICATION TO THE PREDIS PLATFORM

Hoang-Anh Dang, Sana Gaaloul, Benoit Delinchant, and Frederic Wurtz
G2Elab, Grenoble University, Grenoble, France

ABSTRACT

This paper presents the first step modelling process of a smart building in order to ensure better energy management and human comfort in buildings. It consists on combining physical models and experimental measurements in order to have more adapted models for virtual simulation and optimal control. Advantages and difficulties related to this process will be detailed through a defined use case of a smart building: PREDIS.

The paper starts, by introducing the studied building and its different components: HVAC system and thermal envelope. Each one is modelled and validated with measurement data.

INTRODUCTION

Nowadays, building's power consumption represents the most important portion of the global consumption (60% - 70% in France). To reduce this consumption, more efficient energy sources and better insulation are needed. Moreover, building's energy management is more and more required. This require reduced models that are accurate enough. That is why; physical models and experimental measurements will be combined. This modelling process will be applied to the PREDIS smart building.

PREDIS is a complex of several platforms dedicated for research and education. These platforms gather many industrials and academic partners working around emerging axes of electrical engineering and energy management.

In our study, we will focus on the smart building platform called PREDIS smart building. PREDIS SB¹ is a platform installed in G2elab² laboratory, which is used for research activities that are developed around:

- Multi-sensor monitoring
- User activities and their energy impact analysis
- Multi-physical modelling, measurement handle and sensitivity analysing
- Optimal control strategies development.

PREDIS SMART BUILDING

Architecture

PREDIS SB⁽¹⁾ was constructed inside another building (Figure 1). The "building inside a building"

concept could reduce direct external factors (wind and solar) impact to the building.



Figure 1 PREDIS Smart Building

In fact, PREDIS SB has been renovated from an old building by walls insulation improvement and HVAC dual flow. The main thermal insulation is cellulose wadding (14 cm), which was installed on a wooden cladding that surrounds both interior and exterior walls of the platform. However, the intermediate floor composition was unchanged as part of the original foundation.

Materials and HVAC system have been chosen so that the building's maximal energy consumption did not exceed 50kWhPE (Primary Energy)/year.m², in order to respect low energy buildings restrictions.

The first floor of this building, our experimental researches local, is composed of two rooms: computer room and researcher office (Figure 2). The computer room is used for training courses of Grenoble University and equipped with laptops which are connected to the electrical grid and photovoltaic generators. The researcher office, where the control, supervision and measurement are installed, is daily occupied by about six researchers.



¹ SB: Smart Building

² G2Elab: Grenoble Electrical Engineering Laboratory

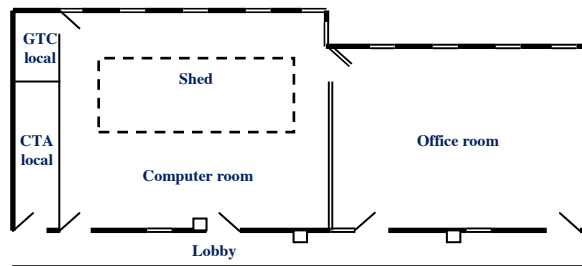


Figure 2 Computer room and office room

To benefit from natural light, windows are installed around the platform and on the ceiling of the computer room. In the office room, at the darker area, a lighting tube is positioned in the middle of the area to save electrical lighting consumption. According to the thermal insulation standard, the window type must be double-glazing.



Figure 3 Shed and lighting tube

Lighting system

The lighting system is necessary to control the brightness when occupant works under less sunlight condition and especially in the evening. Each room is separated into two zones: the first day area (near window side) and the second day area (office side), in order to have light dimming according to natural solar irradiance.

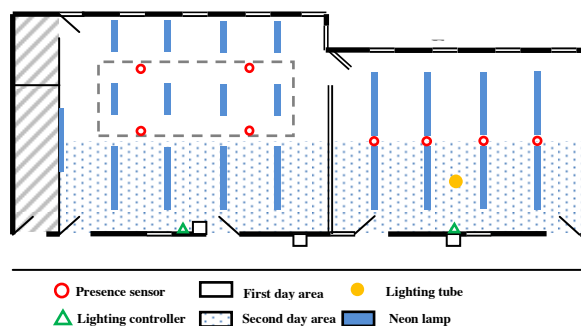


Figure 4 Lighting plan

The lighting control is achieved by the combination of presence and light sensors grid. First, the light is activated by a presence sensor, which detects the first movement that appears in the room. Then, the lighting controller decides how to provide electrical power for each zone in two operating modes: manual mode and automatic mode.

- A short touch can control ON/OFF to the artificial lighting (manual mode).
- A long touch can increase or decrease gradually lighting according to its desires (manual mode). Then, this configuration will be saved as a set point for next lighting activation (automatic mode).

Moreover, the lighting management can be configured according to schedule or periods of occupation.

Standby mode engages after 15 minutes of non-presence in detection area. After this interval time, the system will automatically turn off the lights.

PREDIS HVAC system

As follows the architectural description, a heating ventilation and air conditioning (HVAC) system is essential for PREDIS SB to maintain comfort temperature since no zone heating device is installed. Its role is to ensure fresh air inside the platform and save power heating/cooling energy by heating exchange between incoming and outgoing airflow. If the exhaust air temperature is the lower than the set point temperature, the hot water heating is turned on.

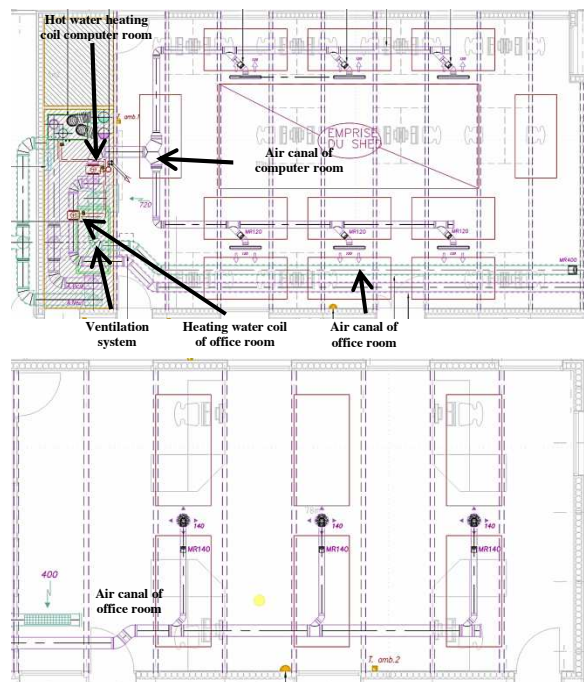


Figure 5 HVAC system plan

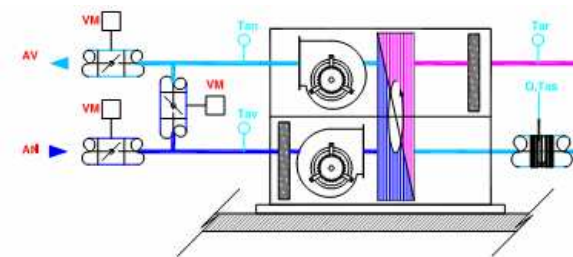


Figure 6 Ventilation double airflow system

The HVAC is decomposed as follow:

Electrical part:

The electrical part contains two variable speed drives and two induction motors associated with the extraction and blowing air. Its performances are linked to the control mode configured in the speed drive.



Figure 7 Induction motors and variable speed drivers

Aeraulic part:

The aeraulic part is made of a centrifugal type fan which drives the airflow in tubes.

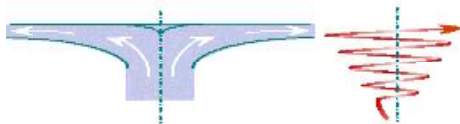


Figure 8 Centrifugal fan

Thermal part:

The thermal part includes a rotary heating exchanger and two hot water heating coils. Each heating coil controls the temperature of each room (computer room and office room).

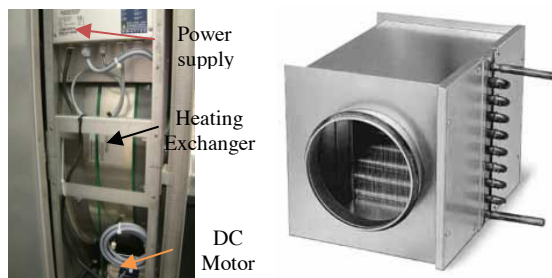


Figure 9 Rotatory heating exchanger and hot water heating coil

Temperature sensors grid

To survey ambient temperature inside and around the platform, two sensor systems are installed. A monitoring system measures the outside air temperature and airflow temperature inside HVAC system. An other monitoring system (Oregon Scientific) has been implemented according to the demand of researchers to study the partial ambient temperatures of the platform, which are important to validate thermal models.

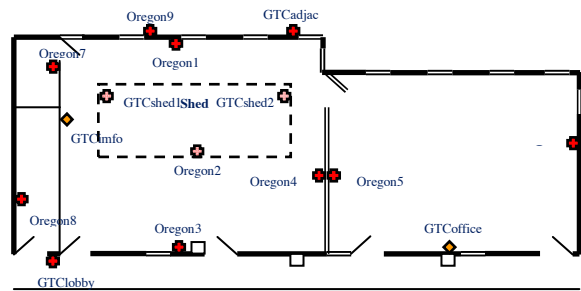


Figure 10 Temperature sensors grid

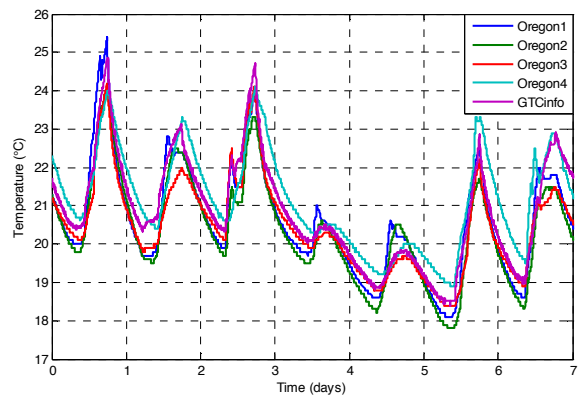


Figure 11 Temperature measurement of computer room

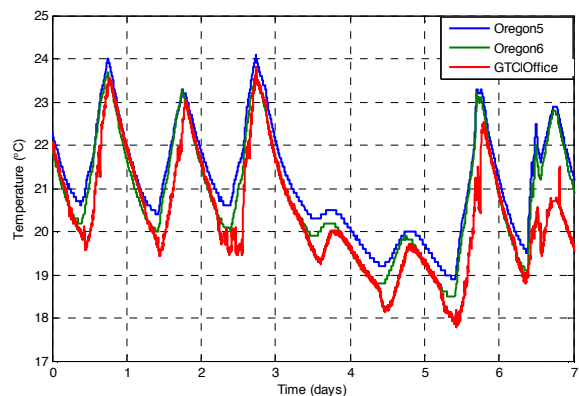


Figure 12 Temperature measurement of office room

Management and Monitoring system

The system ensures building's technical equipments to be managed on:

- Heating, Ventilation and Air Conditioning system (HVAC system)
- Lighting control
- Experimental instrumentation: temperature sensors, airflow sensors, CO₂ sensors, energy meters, switching devices...

Besides, the monitoring system offers the possibility to visualize all measured data and to define set points (Figure 13).

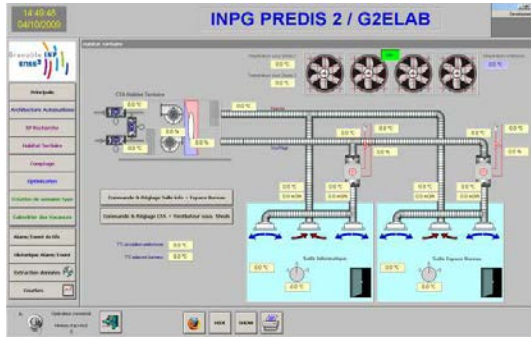


Figure 13 Management and Monitoring System

MODELLING AND MEASUREMENT VALIDATION

PREDIS HVAC system

The aeraulic model, which represents relation of airflow to fan resistance torque, is identified by measurement data.

Quadratic relation of fan rotatory speed (rpm) to motor resistance torque (Nm) (fan model) (e.g. DANG et al., 2010) is defined by equation (1):

$$C = 1.25 \times 10^{-7} \times \Omega_R^2 \quad (1)$$

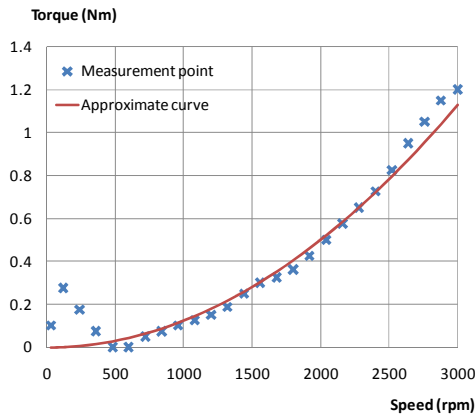


Figure 14 Comparison between measured and estimated torque in term of rotatory speed

Linearly relation of airflow (m^3/h) to fan rotatory speed (rpm) (air canalisation model) at nominal point following the fan law: "Flow is proportional to shaft power":

Blowing airflow:

$$\omega_{R_blowing} = \frac{2916}{1800} Q_{blowing_air} \quad (2)$$

Recovery airflow:

$$\omega_{R_recovery} = \frac{2924}{1200} Q_{recovery_air} \quad (3)$$

Regarding electrical part (e.g. DANG et al., 2010), its model is made for power consumption evaluation and parameterized from constructor data.

The induction motor model is based on an equivalent electrical circuit. From resistance torque calculated by aeraulic model, it allows calculating joule losses and power consumption.

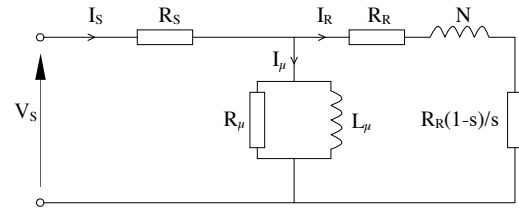


Figure 15 Induction motor equivalent circuit in permanent operation

Mechanical power:

$$P_{mec} = I_R^2 \cdot R_R \frac{1-s}{s} = C \cdot \omega_R \quad (4)$$

Power consumption:

$$P_{motor} = V_S I_S \cos \varphi \quad (5)$$

Joule losses:

$$Joule\ losses = P_{motor} - P_{mec} \quad (6)$$

The variable speed drive controls motor speed rotation by supplying input voltage and frequency to the induction motor. By studying its structure of power electronic circuit, its operational losses are described as below:

Conduction losses:

- IGBT (insulated-gate bipolar transistor):

$$\Delta P_{IGBT_cond} = V_{CE0} I_{IGBTmoy} + R_{IGBT} I_{IGBTeff}^2 \quad (7)$$

- Anti-parallel diode:

$$\Delta P_{d_cond} = V_{d0} I_{dmoy} + R_d I_{deff}^2 \quad (8)$$

Switching losses:

- IGBT (insulated-gate bipolar transistor):

$$W_{on} = \frac{W_{onref}}{E_{ref} \cdot I_{ref}} \cdot E \cdot I \quad W_{off} = \frac{W_{offref}}{E_{ref} \cdot I_{ref}} \cdot E \cdot I \quad (9)$$

- Anti-parallel diode:

$$W_{d_com} \approx W_{doff_com} = I_d \frac{Q_{rr_ref}}{I_{d_ref}} E \quad (10)$$

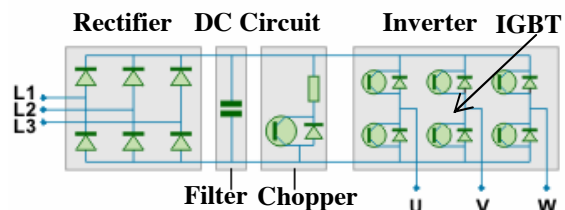


Figure 16 Power electronic circuit of speed drive

To check the accuracy of this model, the calculated energy consumption of HVAC system is compared to measured data.

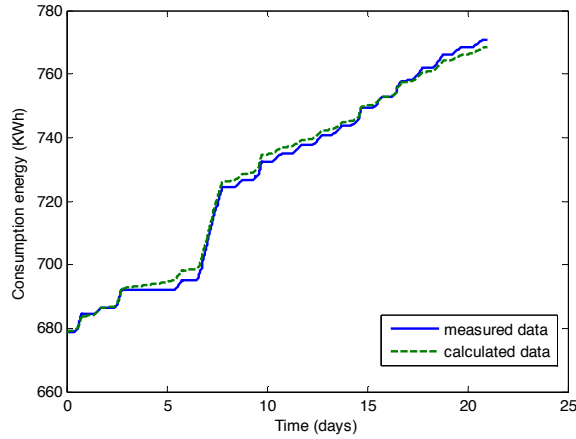


Figure 17 Comparison of electrical energy consumption

Toward the thermal part, the rotary heat exchanger is modeled using the NTU⁽³⁾, using heating power exchanged between in-coming and out-coming air and also new air temperature after this exchange (e.g. Wetter, 1999).

$$\varepsilon = f(NTU, C = \frac{C_{min}}{C_{max}}, kind) \quad (11)$$

This method was adapted due to a correlation with a counterflow static exchanger kind, in order to take into account rotation terms (e.g. Kays, 1984).

$$\varepsilon = \varepsilon_{cc} \left(1 - \frac{1}{9(C_r^*)^{1.93}} \right) \quad (12)$$

$$C_r^* = \frac{C_r}{C_{min}} = \frac{M \cdot c_m \cdot N}{C_{min}} \quad (13)$$

After parameters and nominal variables identification, results were compared to measurements data (Figure 18). Some differences can be explained by sensors precision or aeraulic circuit infiltrations (opened doors or windows).

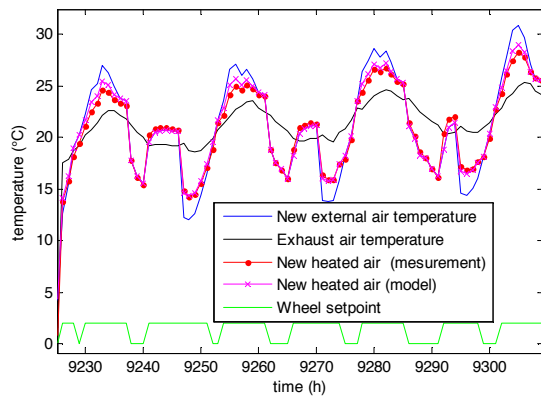


Figure 18 In-coming heated air temperature after the rotary heat exchanger: model and measurement comparison

NTU method was also used for hot water heating coil modelling. A comparison between simulations and measurements is also done (Figure 19):

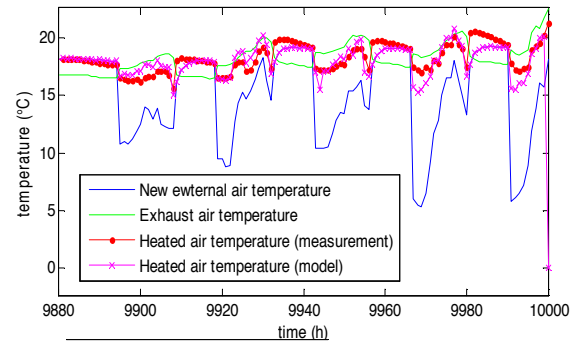


Figure 19 In coming heated air temperature after the hot water heating coil: model and measurement comparison

Thermal building envelope

The thermal envelope is modelled by using an electrical equivalent circuit (Figure 22) (Figure 23) (e.g. Hadsen et al., 2010). It models ambient temperature evolution by solving a state system, in which, the wall temperature is the state variable and the matrix input relates to internal thermals sources and temperature around the platform:

$$\frac{\partial T_{wall}}{\partial t} = A T_{wall} + B u(t) \quad (14)$$

$$T_{int} = C T_{wall} + D u(t)$$

The platform thermal envelope is defined by the coupling of two room thermal models (computer room and office room) (Figure 22) (Figure 23). Only one capacity is used per zone for fast simulation and easier identification procedure.

The parameters need to be identified from materials and architectural description (Figure 24). Their values are firstly estimated for initialisation by analytical calculation:

$$R_{wall_analytic} = \frac{e}{\lambda \cdot S} \quad (15)$$

$$C_{wall_analytic} = \rho \cdot e \cdot S \cdot C_p$$

The airflow equivalent resistance is calculated using equation (16):

$$R_{air} = \rho_{air} \cdot Q_{air} \cdot C_{p_air} \quad (16)$$

After that, those values are calibrated by error minimisation between calculated and measured ambient temperature.

³ NTU: Number of Transfer Units

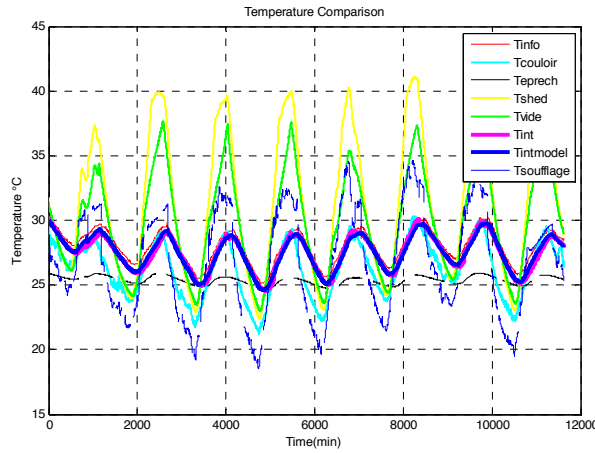


Figure 20 Comparison of ambient temperature in offices room

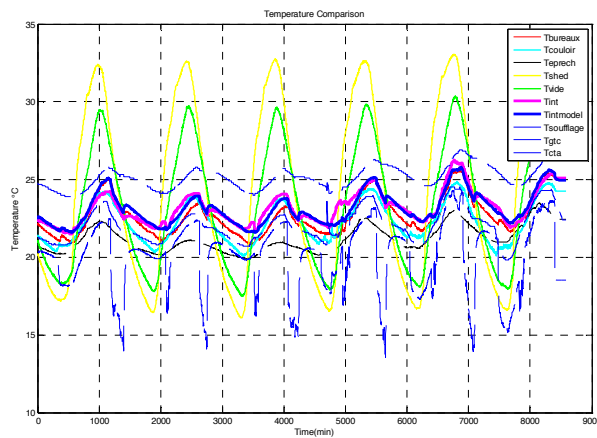


Figure 21 Comparison of ambient temperature in computer room

Parameters of each room thermal model are identified at different period in order to avoid as much as possible any unnecessary occupant activity and lack of measurement.

CONCLUSION

The modelling of PREDIS smart building has been investigated in order to perform researches on building energy management and optimal control. The global model is required to predict the energy consumption and human comfort following proposed scenario. Moreover, those models are not only accurate for simulation but also used for optimisation. Furthermore, they can be used as a sizing tool for designing a virtual building before construction.

In this paper, we present the modelling of HVAC system and thermal envelope, which are used to calculate electrical energy consumption for ventilation and ambient temperatures evolution inside this platform. This work is our first step to reach the PREDIS SB global model.

At this time, our global model is nearly completed and need to be coupled with electrical laptop management model, air comfort control model and temperature comfort control model, which are

developed and being checked regarding measurements.

This modelling work is offering many research perspectives for our group in the field of energy management systems including user interactions and predictive control.

NOMENCLATURE

- C = Mechanical torque (Nm)
- Ω_R = Rotatory speed (rpm)
- V_s = Motor voltage (V)
- R_s = Stator resistance (Ω)
- I_μ = Magnetisation current (A)
- R_μ = Magnetisation resistance (Ω)
- L_μ = Magnetisation inductance (H)
- R_R = Rotor resistance (Ω)
- N = Equivalent inductance (H)
- s = slip
- P_{mec} = Mechanical power (W)
- ω_R = rotatory speed (rad/s)
- P_{motor} = Motor power consumption (W)
- V_{CE0} = IGBT threshold voltage (V)
- $I_{IGBTmoy}$ = IGBT average current (A)
- R_{IGBT} = IGBT resistance (Ω)
- $I_{IGBTeff}$ = IGBT effective current (A)
- V_{d0} = Diode threshold voltage (V)
- I_{dmoy} = Diode average current (A)
- R_d = Diode resistance (Ω)
- I_{deff} = Diode effective current (A)
- $W_{on} W_{off}$ = IGBT Switching on/off energy (J)
- E_{ref}, I_{ref} = IGBT Reference Voltage/Current DC (A)
- E, I : IGBT Voltage/Current DC (V)
- I_d = Diode current (A)
- I_{d_ref} = Diode reference diode current (A)
- Q_{rr_ref} = Diode reference reverse recover charge (C)
- E = Diode voltage DC (V)
- ϵ : efficiency
- C_{min} : minimal heat capacity (J/°K)
- C_{max} : maximal heat capacity (J/°K)
- M : wheel mass (kg)
- N : wheel rotation speed (tr/s)
- C_m : specific heat of the wheel material (J/kg·°K)
- T_{wall} = Equivalent wall temperature (°C)
- T_{int} = Inside ambient temperature (°C)
- $R_{wall_analytic}$ = Analytical calucalted wall resistance (W/°K)
- e = wall thickness (m)
- λ = thermal conductivity (W/(m.K))
- S = wall surface (m²)
- $C_{wall_analytic}$ = Analytical calucalted wall capacitance (J/°K)
- ρ = masse density (kg/m³)
- C_p = specific heat (J/(kg.K))

REFERENCES

Dang, H.A., Delinchant B., Wurtz F. 2010. Electrical performance optimization of an HVAC dual flow Electrimac 2010 Conference, Paris, France.

M. Wetter, "Simulation Model Air-to-Air Plate Heat Exchanger », Laboratoire Nationale de Lawrence Berkley, January 1999.

W. M. Kays, A. L. London, « Compact Heat Exchangers », McGraw-Hill, 1984.

M. Wetter, « Simulation Model Finned Water-to-Air Coil Without Condensation », LNBL, January 1999

Hadsen, M., Bacher, P., Delff Ph., 2010. Building energy performance – Model identification and parameter estimation, Informatics and Mathematical Modelling, Technical University of Denmark.

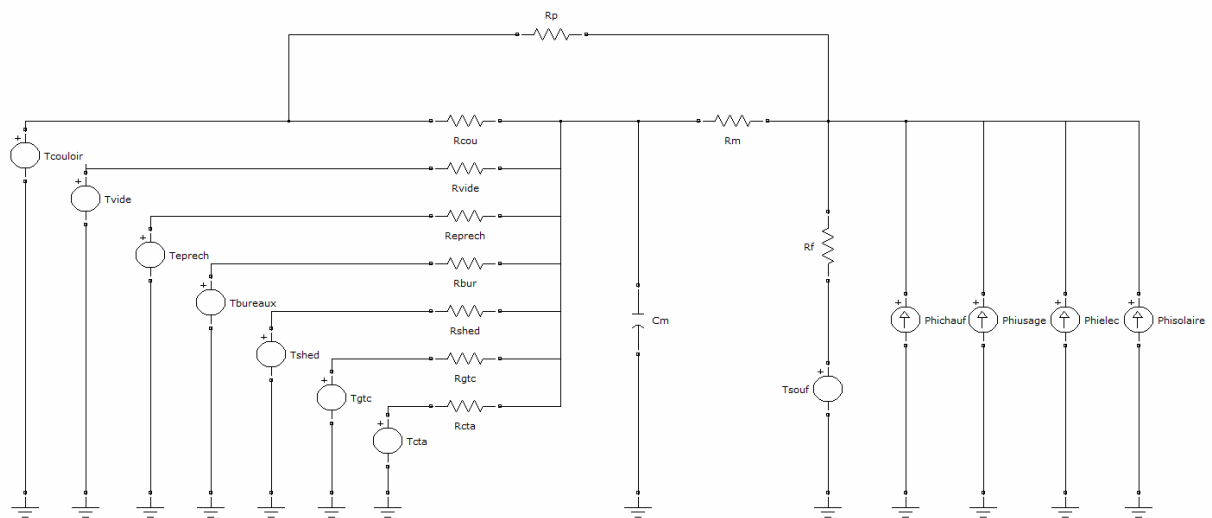


Figure 22 Thermal model of computer room

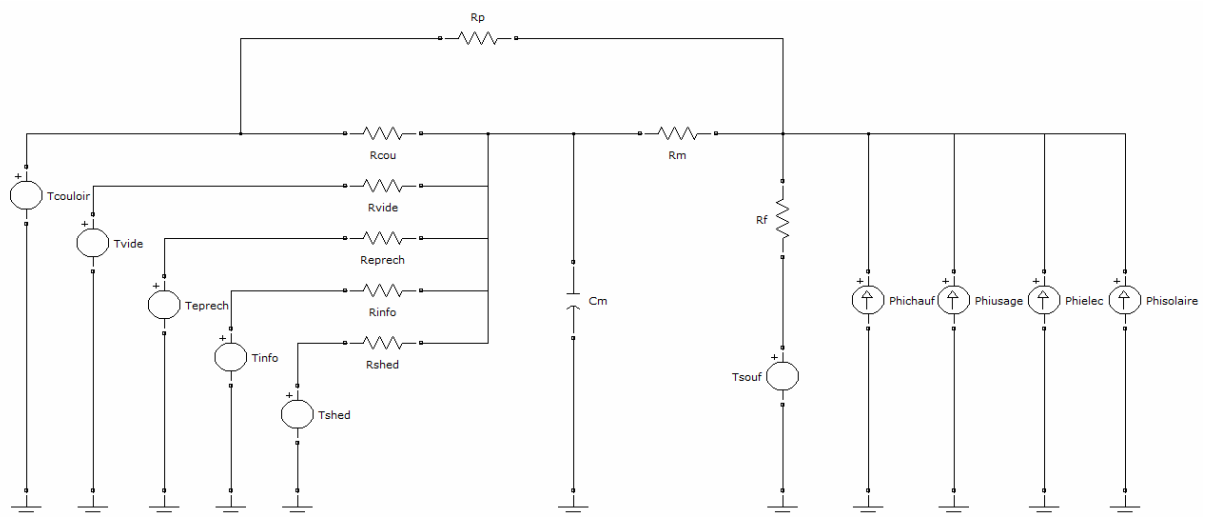


Figure 23 Thermal model of offices room

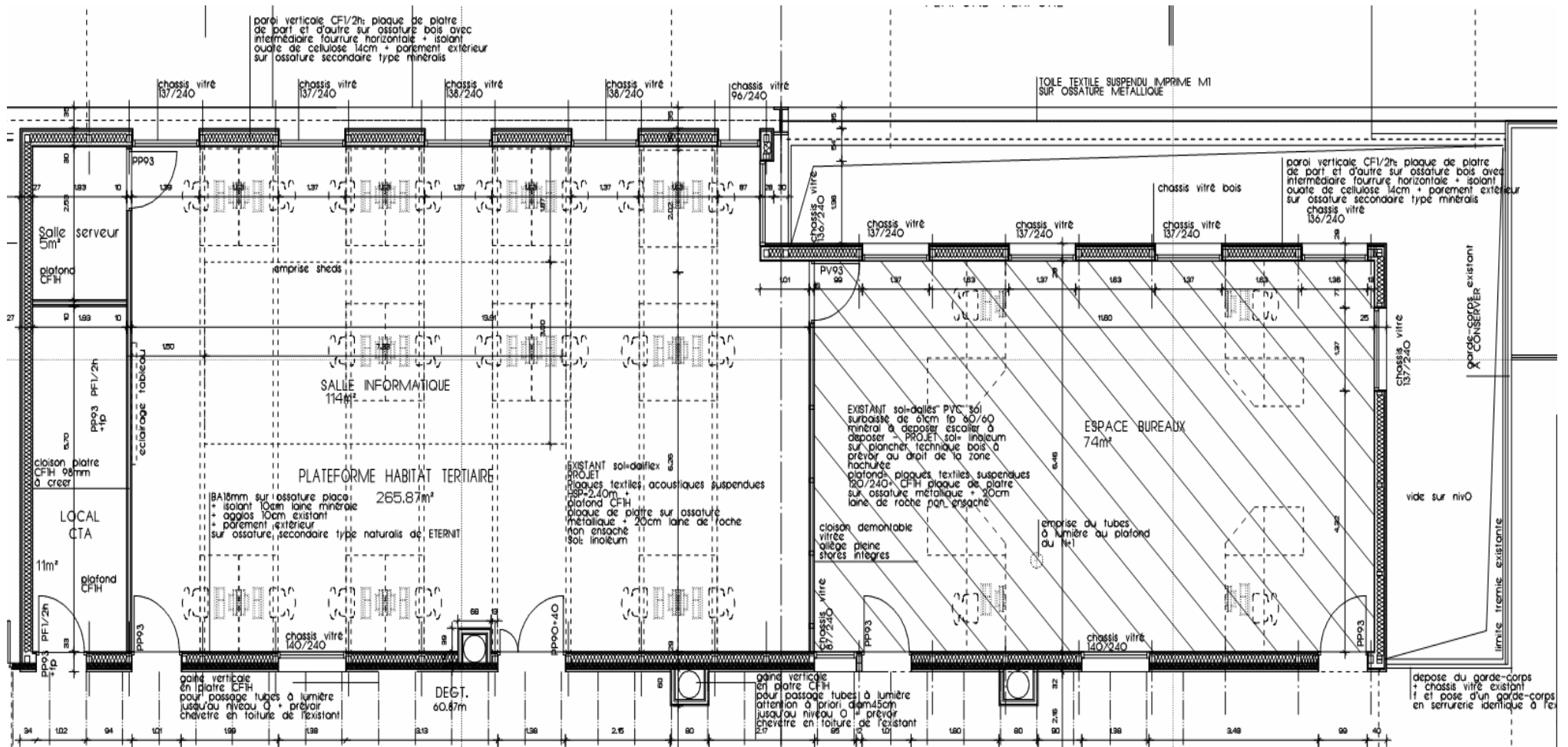


Figure 24 PREDIS SB architectural plan